jp1118579

DATASET · JANUARY 2014

3 AUTHORS, INCLUDING:

Norifusa Satoh

National Institute for Materials Science

23 PUBLICATIONS **681** CITATIONS

SEE PROFILE

THE JOURNAL OF PHYSICAL CHEMISTRY C

ARTICLE

pubs.acs.org/JPCC

Injection Efficiency in Dye-Sensitized Solar Cells within a Two-Band Model

Jinhua Cai,[¶,†,‡] Norifusa Satoh,[†] and Liyuan Han*[,†,‡]

[†]Advanced Photovoltaics Center, National Institute for Materials Science, Tsukuba, Ibaraki 305-0047, Japan, and

[‡]CREST, Japan Science and Technology Agency, Tokyo 102-0075, Japan

ABSTRACT: The injection efficiency in dye-sensitized solar cells is investigated theoretically within a general two-band model, which consists of a conduction band in semiconductor anode and an energy level for the lowest unoccupied molecular orbit (LUMO) in dye molecule. Formulas for the calculation of injection efficiency are derived by using a thermodynamical statistics on the injection current at steady state. The dependence of injection efficiency on various electronic structure parameters, such as the LUMO level relative to conduction band edge, density of states, and so forth, is examined. An approximate expression is obtained for a qualitative description of injection efficiency in the dye-sensitized solar cell operated at a normal conditions. Our results demonstrate that the thermodynamical competition between forward transfer current (from LUMO level to conduction band) and backward transfer current (from conduction band to LUMO level) should be considered in the evaluation of injection efficiency, and the competition results in a lower injection efficiency than unity. The previous experimental results on injection efficiency, such as the weak electron density dependence (or bias dependence), the effect of LUMO delocalization, and so forth, can be well interpreted by using our formula.

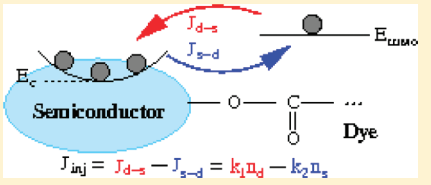

INTRODUCTION

The dye-sensitized solar cell (DSC) has attracted much attention due to its rather high efficiency and low cost.[1] The photovoltaic performance of DSC is mainly determined by four processes, namely light absorption by dye molecule, electron injection from excited dye to nanocrystal semiconductor anode, electron diffusion in the anode, and electron recombination through the interface of semiconductor/dye/electrolyte. Because the electron injection has shown a subpicosecond behavior,[2−5] which is much faster than the competing process of exited state decay to ground, in TiO_2/Ru-bipyridyl dye films coated in inert solvent, it has not generally been considered to be a key factor limiting device performance, and hence much optimization effort has been focused upon light absorption, electron diffusion, and electron recombination. However, the injection dynamics has been found to depend on the chemical environment[6,7] and an injection time slower than a subpicosecond has been confirmed in a complete DSC[8] and in a film.[9] In recent years, some experimental evidence has revealed a lower injection efficiency than unity in DSC, and various parameters influencing the injection efficiency have been investigated.[8,10,11]

In comparison with those experimental works on injection process, the theoretical investigation is scarce. The previous theoretical works are mainly focused on the direct calculation of rate constant[12] and electron transfer dynamics[13] at the ab initio level. Because the electron injection occurs between the excited dye and semiconductor anode, the injection efficiency should be determined by the electronic structures of dye molecule and semiconductor. Currently, there are not any explicit expressions to describe injection efficiency from electronic structure parameters at a level of model. In literature, the formula[14]

$$k_{inj} = \frac{2\pi}{\hbar}\int dE\rho(E)|V(E)|^2 \qquad (1)$$

or its variation[7,15,16] was often used for the interpretation of injection rate constant. A finite injection efficiency lower than unity was interpreted as a result of assumed conduction-band-fluctuation[17] (site heterogeneity[18]) or a LUMO level splitting[14] due to molecular vibration. In the previous approaches,[14,17,18] the LUMO level was usually regarded as an injection source; however, its potential role as an acceptor has not been considered except in the case with a LUMO level lower than the conduction band edge.[19] When the LUMO level with a finite expansion due to molecular vibration is near the conduction band edge, the backward transfer current (from conduction band to the LUMO level) may be a critical factor to determine the magnitude of injection efficiency, especially in the situation where intramolecular decay shows a time constant much larger than injection time. In this article, we start from a thermodynamical statistical description for injection current within a general two-band model, a set of formulas for the calculation of injection efficiency is derived, and the dependence of injection efficiency on various electronic structure parameters are discussed with the relevant experimental results. We will see that the thermodynamical competition between the forward transfer current and the backward transfer current naturally leads to a finite injection efficiency, which can

Received: December 14, 2010
Revised: February 1, 2011
Published: March 07, 2011

dx.doi.org/10.1021/jp1118579 | J. Phys. Chem. C 2011, 115, 6033–6039

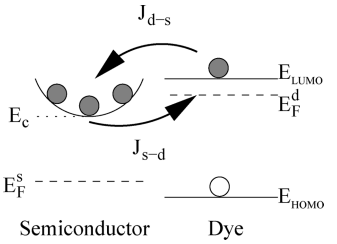

Figure 1. Schematic diagram for the energy level configuration within a general two-band model. Under illumination, an electron transits to LUMO level and a hole is left on the highest occupied molecular orbit (HOMO) level in dye. The electron has same probability for the forward transition from the LUMO level to the state in the conduction band as that for the backward transition. The actual injection current is determined by the competition between the backward transfer current (J_{s-d}) and the forward transfer current (J_{d-s}).

be described by an explicit formula containing electronic structure parameters of dye molecule and semiconductor. Because the thermodynamical competition always exists in the injection process, the actual injection efficiency cannot exceed the value estimated from our formula whether for a fast injection or a slow injection.

MODEL AND FORMULAS

Two-Band Model and Density of States. Prior to formula derivation, a general two-band model for injection is introduced. This model consists of two bands, the one is the conduction band in semiconductor, the other is the LUMO level with a finite expansion due to molecular vibration, which is characterized by a Lorentz-type state density (Figure 1 for energy level configuration). This is a minimal configuration for the modeling of electron injection because only one competition process (electron transition from conduction band to LUMO level) is considered. This is valid in the case where the injection process possesses a larger rate constant than other competition processes, for example, the decay of excited state to ground state in dye molecule.

To perform an actual calculation, we need to provide the concrete form of state density. We use the following state density

$$\rho_s(E) = \begin{cases} N_l \exp\left[\alpha_l(E - E_c)/k_B T\right] & (E \le E_c) \\ N_l + 4\pi\left(\dfrac{2m_{eff}}{h^2}\right)^{3/2}(E - E_c)^{1/2} & (E > E_c) \end{cases} \quad (2)$$

for the conduction band in oxide semiconductor. An effective mass approximation is adopted for the state density above the conduction band edge E_c, and m_{eff} is the effective mass of conduction band electron. An exponentially decayed tail is augmented to the ideal conduction band, and the parameters N_l and α_l^{-1} are used to characterize the strength and distribution width of localized states in gap,[20] respectively.

For the LUMO level in dye molecules, we use a Lorentz type of state density

$$\rho_d(E) = \frac{1}{\pi}\frac{g\Gamma}{(E - E_{LUMO})^2 + \Gamma^2} \quad (3)$$

where Γ is the Lorentz expansion due to molecular vibration and g is a factor to characterize the magnitude of state density (number of LUMO level per volume).

Derivation of Formulas for Injection Efficiency. According to thermodynamical statistics, the transition current from the excited dye molecule to oxide semiconductor is[21]

$$J_{d-s} = T_{d-s}\int dE\rho_s(E)\rho_d(E)[1 - f_{E_F^s}(E)]f_{E_F^d}(E) \quad (4)$$

Here, T_{d-s} is quantum transition probability of electron from the lowest unoccupied molecular orbit (LUMO) in dye molecule to the conduction band in oxide semiconductor. The $\rho_d(E)$ and $\rho_s(E)$ denote the state densities in dye molecule and in oxide semiconductor, respectively. The $f_{E_F}(E)$ is Fermi−Dirac distribution function, and E_F^s (E_F^d) is the quasi-Fermi energy level for the nonequilibrium electrons in oxide semiconductor (dye molecule). In a general situation, T_{d-s} is a function of energy E. Considering on the fact that $\rho_d(E)$ for LUMO level usually exhibits a peak around E_{LUMO}, we can use an average value around E_{LUMO} instead of $T_{d-s}(E)$ and move it out of integral.

Similarly, the transition current from the oxide semiconductor to dye molecule is

$$J_{s-d} = T_{d-s}\int dE\rho_s(E)\rho_d(E)[1 - f_{E_F^d}(E)]f_{E_F^s}(E) \quad (5)$$

Because the quantum transition probability for back transfer process is the same as that for the forward transfer process, here we use T_{d-s} directly instead of T_{s-d}.

The net injection current $J_{inj} = J_{d-s} - J_{s-d}$, so

$$J_{inj} = T_{d-s}\int dE\rho_s(E)\rho_d(E)[f_{E_F^d}(E) - f_{E_F^s}(E)] \quad (6)$$

With an introduction of

$$n_{s(d)} = \int dE\rho_{s(d)}(E)$$
$$k_1 = T_{d-s}\int dE\rho_s(E)\rho_d(E)f_{E_F^d}(E)/n_d$$
$$k_2 = T_{d-s}\int dE\rho_s(E)\rho_d(E)f_{E_F^s}(E)/n_s \quad (7)$$

J_{inj} is written as

$$J_{inj} = k_1 n_d - k_2 n_s \quad (8)$$

where $k_{1(2)}$ is forward (backward) transfer rate constant, n_d and n_s are electron densities on LUMO level of dye molecule and in conduction band of oxide semiconductor, respectively.

The injection occurs between two distinct regions, the one is in dye molecule and the other is in semiconductor, so the electrons participating an injection process occupy different space with different volume. Suppose that the volume of the occupied space in dye is V_d and that in semiconductor is V_s, and that the contact area of dye molecule with semiconductor is A, then we have a set of kinetic equations

$$\left(\frac{V_d}{A}\right)\frac{\partial n_d}{\partial t} = -J_{inj}$$
$$\left(\frac{V_s}{A}\right)\frac{\partial n_s}{\partial t} = J_{inj} \quad (9)$$

with initial condition

$$n_d(t = 0) = n_{d0}$$
$$n_s(t = 0) = n_{s0} \quad (10)$$

dx.doi.org/10.1021/jp1118579 |J. Phys. Chem. C 2011, 115, 6033–6039

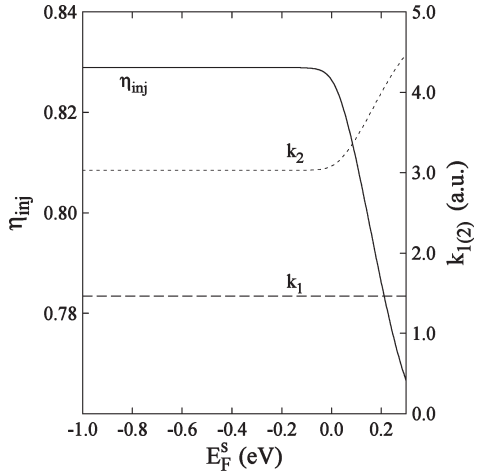

Figure 2. Injection efficiency η_{inj}, rate constants k_1 and k_2 as functions of quasi-Fermi energy level E_F^s in semiconductor. For the frequently used anatase TiO_2, the effective mass $m_{eff} = 1.0\ m_e$ (m_e is the mass of electron) is adopted. Here, an ideal conduction band is considered, so parameter $N_l = 0$. For dye molecule, $E_{LUMO} = 0.3$ eV, $\Gamma = 0.3$ eV, $E_F^d = 0.3$ eV, and $g = 5.0\ nm^{-3}$ are assumed. The geometry factor $f_g = 0.1$ is adopted. The conduction band edge (E_c) is set as the zero point of energy.

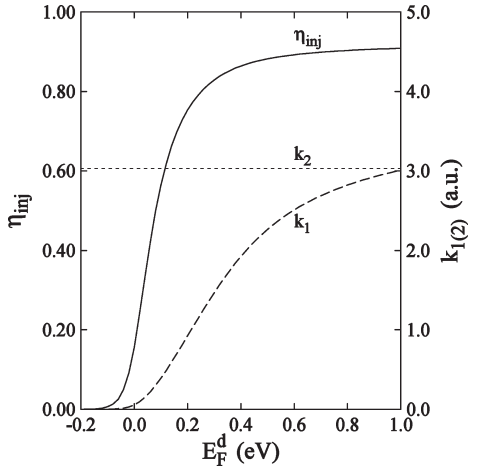

Figure 3. Injection efficiency η_{inj}, rate constants k_1 and k_2 as functions of quasi-Fermi energy level E_F^d in dye molecule. $E_F^s = -1.0$ eV, and other parameters are the same as in Figure 2.

to describe the evolution of electron density in injection process. If k_1 and k_2 are constants independent of electron density, the above equations degenerate into a set of first-order linear equations, and the injection efficiency can be calculated from expression

$$\eta_{inj} \equiv 1 - \frac{n_d(\infty)}{n_{d0}} = \frac{1 - (f_i k_2/k_1)}{1 + (f_g k_2/k_1)} \tag{11}$$

where $f_i = n^{s0}/n^{d0}$ (a dimensionless factor related to initial condition) and $f_g = V^d/V^s$ (a dimensionless geometry factor). Usually $n^{s0}/n^{d0} \ll 1$, so the above expression can be simplified as

$$\eta_{inj} = [1 + (f_g k_2/k_1)]^{-1} \tag{12}$$

The factor f_g in the above expression characterizes the effect of size on injection efficiency. A simple estimation of f_g is L^d/R where L^d is the length of dye molecule and R is the radius of nanocrystalline grain. This estimation is valid in the situation where the semiconductor grain has a high crystallinity, and the size of grain becomes a main factor to determine how much space in semiconductor is involved in injection process. Because of this geometry limitation, the injection efficiency will increase with grain size[22] if density of states is fixed. In a typical ruthenium DSC, $L^d \approx 1$ nm and $R \approx 10$ nm, so f_g is about 0.1. In following calculation, we will adopt this value for f_g. It should be mentioned here that eq 11 or eq 12 will not be an exact expression, and become an approximate one when k_1 and k_2 depend on electron density.

Approximate Expression for Injection Efficiency. Formulas in eq 7 are suited to numerical calculation but not convenient for us to understand the physical mechanism relevant to injection efficiency. Considering on the characteristic of state densities in our model, we derive a set of approximate expressions for k_1 and k_2. Because ρ_d exhibits a sharp peak around E_{LUMO}, the integral for k_1 in eq 7 is most contributed by the values around E_{LUMO}, and

$$k_1 \approx T_{d-s}\rho_s(E_{LUMO}) \tag{13}$$

This approximation holds for E_F^d in the vicinity of E_{LUMO} and for a narrow LUMO state density, otherwise an averaged energy E_{av} on LUMO level should be used instead of E_{LUMO} in eq 13.

The situation for k_2 is a little complicated in comparison with that for k_1 because E_F^s may go across the singularity point of $\rho_s(E)$. For an ideal conduction band ($N_l = 0$),

$$k_2 \approx \begin{cases} T_{d-s}\rho_d(E_c) & (E_F^s \le E_c) \\ T_{d-s}\rho_d(E_F^s) & (E_F^s > E_c) \end{cases} \tag{14}$$

For a cell worked at normal conditions, E_F^s is below E_c, and this yields

$$\eta_{inj} \approx \{1 + f_g[\rho_d(E_c)/\rho_s(E_{LUMO})]\}^{-1} \tag{15}$$

This approximate expression for η_{inj} indicates that the lower value than unity for η_{inj} results from the nonzero state density of LUMO energy level at conduction band edge E_c. This formula provides us an alternative way to understand the origin of finite injection efficiency lower than unity besides the fluctuation of injection energetics.[8,14,17,18]

RESULTS AND DISCUSSIONS

In following context, we will give a thorough investigation on the injection efficiency for various model parameters based on eqs 2, 3, 7, and 12 and discussion with relevant experimental results.

Quasi-Fermi Energy Level Dependence. Figure 2 shows the calculated injection efficiency as a function of quasi-Fermi energy level in semiconductor with an ideal conduction band ($N_l = 0$ in eq 2). The η_{inj} is almost a constant for $E_F^s < E_c$, but it decreases with E_F^s for $E_F^s > E_c$. From the E_F^s dependence of k_1 and k_2, we find that the variation of k_2 is responsible for the E_F^s dependence of η_{inj}. When E_F^s is below E_c, the electrons occupy the states in the vicinity of conduction band edge via thermal excitation, then transit to LUMO level in dye, so the back transfer current is proportional to the electron density (n_s) in conduction band, and a constant k_2 is yielded. When E_F^s is above E_c, the back transfer current is contributed by the electrons at Fermi level, and k_2 increases with E_F^s because the state density of LUMO level also increases with E_F^s.

dx.doi.org/10.1021/jp1118579 |J. Phys. Chem. C 2011, 115, 6033–6039

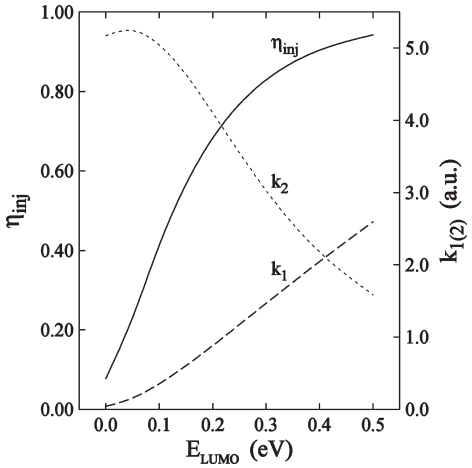

Figure 4. Injection efficiency η_{inj}, rate constants k_1 and k_2 as functions of E_{LUMO} relative to E_c. $E_F^s = -1.0$ eV, $E_F^d = E_{LUMO}$, and other parameters are the same as in Figure 2.

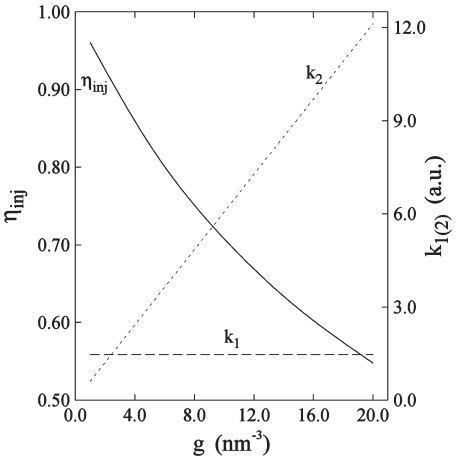

Figure 5. Injection efficiency η_{inj}, rate constants k_1 and k_2 as functions of g. $E_F^s = -1.0$ eV, and other parameters are the same as in Figure 2.

In experiment, the quasi-Fermi energy level E_F^s in semiconductor can be controlled by applying a negative bias voltage V_{bias}. When V_{bias} sweeps from 0 to E_{redox}, the quasi-Fermi energy level $E_F^s$is changed from E_{redox} to 0. Sara E. Koops et al. have observed a bias-voltage-dependent injection efficiency, which first shows a weak reduction from 0.83 at 0 V to 0.81(5) at −0.84 V, then shows a significant reduction to 0.76 at −1.07 V.[8] They assigned this bias dependence to a reduction in the density of unoccupied acceptor states in semiconductor.[8] However, the reduction of state density only holds in the situation of E_F^s below E_c where electrons can only occupy electronic states in the vicinity of E_c due to the limitation of thermal excitation, and the density of unoccupied states in semiconductor increases with $E_F^s$for $E_F^s > E_c$. So, this bias dependence cannot be assigned to the reduction in the density of unoccupied acceptor states. Additionally, the different characteristics of bias voltage dependence for $V_{bias} > -0.84$ V and $V_{bias} < -0.84$ V are difficult to understand on the basis of previous theoretical framework. If a redox energy $E_{redox} \approx -0.84$ eV, which is slightly larger than the value (−0.93 eV) adopted by J. Ferber et al. in their model simulation,[23] is assumed for their sample, the experimental result can be well explained by using our result.

Figure 3 shows the calculated injection efficiency as a function of quasi-Fermi energy level in dye molecule. The η_{inj} initially exhibits a rapid increase, then approaches saturation, whereas E_F^d sweeps from zero to 1.0 eV. When E_F^d is lower than conduction band edge E_c, the accept state density for forward transfer is almost zero, hence the corresponding rate constant k_1 also approaches zero and a lower injection efficiency is obtained. With the further increase of E_F^d, the accept state density for forward transfer also increases, so the forward rate constant k_1 and the injection efficiency η_{inj} increase too. The reason that the injection efficiency approaches a saturation value is that the electron exchange behavior is dominated by electrons around the LUMO level when E_F^d is higher than LUMO level.

In experiment, the quasi-Fermi energy level E_F^d in dye molecule can be controlled by the energy of excitation photon. A high excitation photon energy means that the electrons at HOMO level can transit to the LUMO level with a high vibration energy, so the E_F^d should increase with excitation energy. Moser et al. have observed significant excitation energy dependence of injection efficiency in experiment, and they have explained the dependence by using vibrational hot electron transfer from LUMO level to conduction band.[14] In our two-band model, the vibration effect is taken into account by introducing an expansion parameter Γ for the LUMO level. Although this is a simple approach, the hot electron effect on injection efficiency found in experiment can be well explained by using our result.

LUMO Energy Level Dependence. It is more interesting to examine the injection efficiency at normal operating condition ($E_F^s < 0$). Figure 4 shows the calculated η_{inj} as a function of LUMO energy level E_{LUMO} relative to E_c. The injection efficiency increases with LUMO level, and this behavior is ascribed to the LUMO dependence of rate constants. With the increase of E_{LUMO}, the forward rate constant k_1 increases because the conduction-band-state density near LUMO level becomes larger, simultaneously, the backward rate constant k_2 decreases because the LUMO state density near conduction band edge becomes smaller. The LUMO dependence of η_{inj} can be well explained by using the approximate expression in eq 15.

A widely accepted concept to describe the LUMO level dependence of injection efficiency is driving force. Usually the concept of driving force is related to the density of states in conduction band. With the increase of LUMO level, the state density in conduction band is increased (see eq 1), so a higher injection is obtained. In our approach, the increase of injection efficiency with LUMO level results from both aspects, the one is the increase of $\rho_s(E_{LUMO})$, and the other is the decrease of $\rho_d(E_c)$.

LUMO State Density Dependence. Figure 5 shows the LUMO state density dependence of injection efficiency. For a ruthenium dye, the magnitude of g is estimated about several nm^{-3}. For example, the volume of single N3 dye molecule is 0.78 nm^{-3},[24] and the factor g for triplet states in N3 dye is estimated as $g = (3 \times 2)/(\text{volume of LUMO}) \approx 6/(\text{volume of N3}) \approx 8\ nm^{-3}$. In Figure 5, the g covers a range from 1 nm^{-3} to 20 nm^{-3}, and the η_{inj} decreases with g, whereas the state density of conduction band is fixed. Because the form of state density for LUMO level has not been changed, the forward rate constant k_1 is a constant independent of g. The backward rate constant k_2 linearly increases with g due to an increased LUMO state density. Here, all the dependence of g can be well explained by eqs 13 to 15.

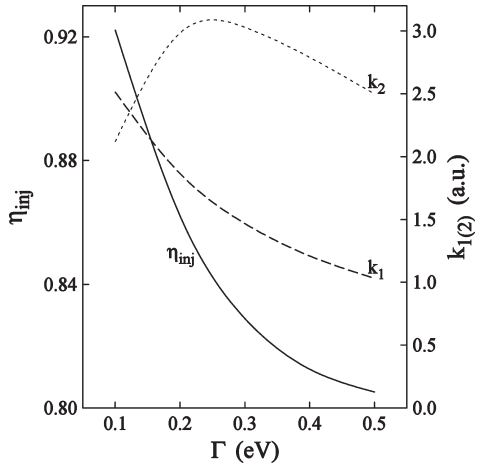

Figure 6. Injection efficiency η_{inj}, rate constants k_1 and k_2 as functions of Γ. $E_F^s = -1.0$ eV, and other parameters are the same as in Figure 2.

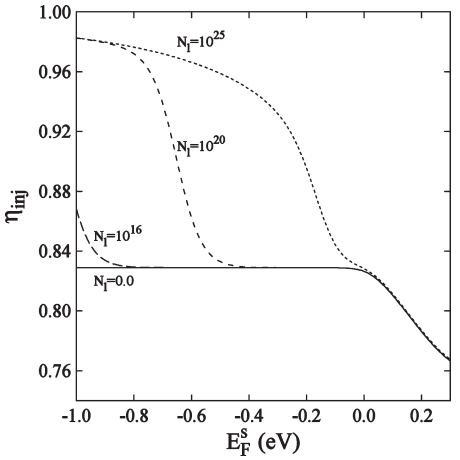

Figure 7. Injection efficiency η_{inj} as a function of quasi-Fermi energy level E_F^s for various N_l. The unit of N_l is m^{-3}, α_l = 0.4 eV, and other parameters are the same as in Figure 2.

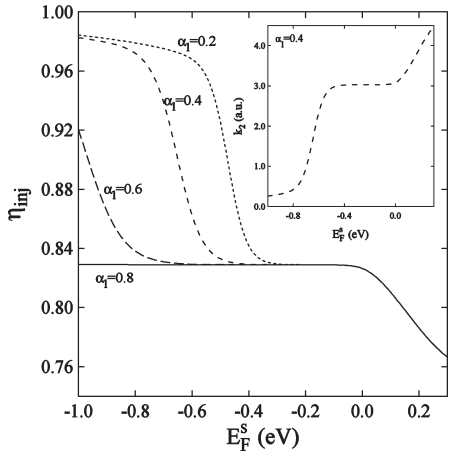

Figure 8. Injection efficiency η_{inj} as a function of quasi-Fermi energy level E_F^s for various α_l. The unit of α_l is eV, $N_l = 10^{20}$ m^{-3}, and other parameters are same as in Figure 2. The insert shows the dependence of k_2 on E_F^s for α_l = 0.4 eV.

The state density dependence of injection efficiency in Figure 5 indicates that tailoring the ratio of ρ_s to ρ_d is an efficient way to adjust injection efficiency. The delocalization of LUMO level in dye is a common strategy to improve the performance of dye, and it can be realized by extending the π-conjugated bridge between donor unit and acceptor unit in dye.[25,26] The delocalization of LUMO level can make the level down shift, and a red-shift occurs in the absorption spectrum, so more solar energy can be absorbed by dye due to a better overlap with solar spectrum. Recently Santos et al. have reported that the injection efficiency is found to be increased by linker conjugation in a series of porphyrin with a free base or zinc central metal, and the state density of LUMO level is more extended in a conjugated dye than in the corresponding nonconjugated dye.[27] This effect of delocalization on injection efficiency may be understood as that (i) the wave function of LUMO state is extended to the anchor group due to delocalization, and a larger overlapping integral between LUMO state and conduction band of semiconductor is obtained, so a faster injection is realized; (ii) the state density around LUMO level is decreased due to delocalization, so the injection efficiency is increased (eq 15). The decrease of state density is realized via dispersion in energy. An extreme example is the energy splitting of degenerate molecular orbit states caused by coupling among these orbit states. Santos et al. has ascribed the enhancement of injection efficiency to the larger overlapping integral due to the delocalization of LUMO level in dye molecule. However, it should be mentioned here that the ratio of injection time to the intramolecular decaying time is almost same whether in a conjugated case or in a nonconjugated case,[27] so there the injection speed may not be a key factor responsible to the enhancement of injection efficiency.

LUMO State Expansion Dependence. Figure 6 shows the dependence of injection efficiency on Lorentz expansion width Γ. With the increase of Γ, more electrons with energy lower than E_{LUMO} in dye transit to conduction band, so k_1 and η_{inj} decrease. The increase of Γ means that the state density of LUMO level is broadened, simultaneously, the peak height is decreased, hence k_2 exhibits a maximum around $\Gamma = E_{LUMO} - E_c$. This leads to a fast decrease of η_{inj} with Γ when Γ is less than $E_{LUMO} - E_c$. The Γ dependence of η_{inj} can also be well explained by using the approximate formula in eq 15 if an average energy E_{av} on LUMO level replaces E_{LUMO} in eq 15.

The nonzero Γ value is a key factor for obtaining a finite injection efficiency lower than unity in our model. If Γ is less than 0.01 eV, the injection efficiency would approach unity. So it is necessary to give an argument about the scale of Γ. The vibration frequencies in dye molecule cover a range of 500 cm^{-1} to 2000 cm^{-1}.[28] For example, the CN group and C═C (C−C) bond are common group/bond in a dye molecule, the stretching vibration of CN group has a scale of 2000 cm^{-1} (0.25 eV),[28,29] and that of C═C (C−C) has a scale of 1600 cm^{-1} (0.2 eV).[28] The electron on LUMO level virtually absorbs or emits phonon, hence a broadened LUMO level is obtained. The actual expansion and the dispersion of state density depend on the electron−phonon coupling strength and distribution of vibration modes. In our two-band model, a Lorentz function is used to model the dispersion of LUMO level, and the parameter Γ is used to characterize the expansion. Because the maximum energy change induced by absorbing or emitting a phonon is about 0.25 eV, a reasonable estimation of Γ is about 0.25 eV, which is larger than the value adopted in the work by R. Katoh et al.[18] Because an efficient injection can be realized only in the

dx.doi.org/10.1021/jp1118579 |J. Phys. Chem. C 2011, 115, 6033–6039

situation of $E_{LUMO} - E_c > \Gamma$, a minimal energy rule emerges. In previous work, the minimal energy rule stems from the assumed site heterogeneity,[18] but here naturally from the LUMO level expansion due to molecular vibration.

Band-Tail State Dependence. Figure 7 and Figure 8 show the dependence of injection efficiency on the band-tail state. For a certain N_l or α_l, a threshold E_F^s is found. When E_F^s is lower than the threshold, the η_{inj} decreases with E_F^s. When E_F^s is larger than the threshold, the dependence shows a behavior as in the situation of an ideal conduction band. This threshold depends on the magnitude (N_l) and distribution width ($1/\alpha_l$) of band tail state, a higher value is obtained for a strong and wide tail.

In order to illustrate the reason why band tail leads to the increase of injection efficiency for a lower E_F^s, we need to examine the E_F^s dependence of $k_{1(2)}$. It is found that k_1 is a constant, so k_2 is responsible for this behavior (insert in Figure 8). When E_F^s is lower than the threshold, the n_s is larger than that in the case of ideal conduction band; when E_F^s is larger than the threshold, more electrons are filled into conduction band via thermal excitation, so n_s approaches the value in the case of ideal conduction band. Because the backward transfer current is determined mainly by the value of joint state density near LUMO level, it is almost same after the augmentation of tail to conduction band. So the band-tail state leads to a decrease of k_2 for a lower E_F^s. A more intuitive interpretation of this effect is that the electrons filled in band tail are trapped and cannot transfer back to LUMO level in dye.

This E_F^s dependence of injection efficiency caused by band tail state has not been observed in experiment. This may be due to following three reasons. The first reason is that the tail is weak or its distribution is narrow. From Figure 7 we find that the injection efficiency for $N_l = 10^{16}$ m^{-3} is almost same as that $N_l = 0$ in the range of -0.8 to 0 eV for E_F^s. The second reason is that there exist fluctuations for N_l and α_l, and average result will show a more weaker E_F^s dependence. The third reason is that there exist some other competition process, such as the electron transfer from the band tail state to the hole on HOMO level in dye. If this E_F^s dependence really exists in some samples, we should be careful to deal with experimental data collected under a weak illumination. For example, the incident-photon-to-current-efficiency (IPCE) is usually measured under weak illumination, we will overestimate the performance of the cell operated under normal illumination by using the IPCE if the impurity state density is high in oxide semiconductor.

It should be mentioned here that the enhancement of injection efficiency due to band tail state is obtained in the situation with a fixed conduction-band-state density. Because the state density of conduction band usually decreases with the increase of band tail state density, the injection efficiency will decrease as whole if the band tail state density is increased. The proper way to increase injection efficiency within this two-band model is to increase the ratio of conduction band density to LUMO state density, not to increase the density of band-tail states.

CONCLUSIONS

In summary, injection efficiency is theoretically investigated within a general two-band model, in which the thermodynamical competition between forward transfer current (from LUMO level to conduction band) and backward transfer current (from conduction band to LUMO level) is considered. The formulas for the calculation of injection efficiency are derived, and an approximate expression $\eta_{inj} = \{1 + f_g[\rho_d(E_c)/\rho_s(E_{LUMO})]\}^{-1}$ is also obtained. Our formulas explicitly relate injection efficiency to electronic structure in oxide semiconductor and dye molecule, and are helpful for us to understand the physics in injection process. Because the thermodynamical competition between the forward transfer current and the backward one always exists, the formulas provide us an estimation of maximum injection efficiency in a real system. In addition to the energy level match, the formulas also imply a way to adjust injection efficiency by tailoring the state density of conduction band in oxide semiconductor and of LUMO level in dye molecule.

AUTHOR INFORMATION

Corresponding Author

*E-mail: han.liyuan@nims.go.jp.

Present Addresses

¶Permanent address: Department of Physics, Shanghai Jiaotong University, Shanghai 200240, China

ACKNOWLEDGMENT

This work was supported by the Core Research for Evolutional Science and Technology (CREST) program of the Japan Science and Technology (JST) Agency. The author (J.C.) thanks Dr. Xudong Yang and Dr. Kun Zhang for helpful discussions.

REFERENCES

(1) O'Regan, B.; Grätzel, M. *Nature* **1991**, *353*, 737.

(2) Asbury, J. B.; Ellingson, R. J.; Ghosh, H. N.; Ferrere, S.; Nozik, A. J.; Lian, T. Q. *J. Phys. Chem. B* **1999**, *103*, 3110.

(3) Benkö, G.; Kallioinen, J.; Korppi-Tommola, J. E. I.; Yartsev, A. P.; Sundström, V. *J. Am. Chem. Soc.* **2002**, *124*, 489.

(4) Ramakrishna, G.; Jose, D. A.; Kumar, D. K.; Das, A.; Palit, D. K.; Ghosh, H. N. *J. Phys. Chem. B* **2005**, *109*, 15445.

(5) Kuang, D. B.; Ito, S.; Wenger, B.; Klein, C.; Moser, J. E.; Humphry-Baker, R.; Zakeeruddin, S. M.; Grätzel, M. *J. Am. Chem. Soc.* **2006**, *128*, 4146.

(6) Bauer, C.; Boschloo, G.; Mukhtar, E.; Hagfeldt, A. *J. Phys. Chem. B* **2002**, *106*, 12693.

(7) Bartelt, A. F.; Schütz, R.; Neubauer, A.; Hannappel, T.; Eichberger, R. *J. Phys. Chem. C* **2009**, *113*, 21233.

(8) Koops, S. E.; O'Regan, B.; Barnes, P. R. F.; Durrant, J. R. *J. Am. Chem. Soc.* **2009**, *131*, 4808.

(9) Kallioinen, J.; Lehtovuori, V.; Myllyperkiö, P.; Korppi-Tommola, J. *Chem. Phys. Lett.* **2001**, *340*, 217.

(10) Barnes, P. R. F.; Anderson, A. Y.; Koops, S. E.; Durrant, J. R.; O'Regan, B. C. *J. Phys. Chem. C* **2009**, *113*, 1126.

(11) Katoh, R; Kasuya, M.; Kodate, S.; Furube, A.; Fuke, N.; Koide, N. *J. Phys. Chem. C* **2009**, *113*, 20738.

(12) Lanzafame, J. M.; Miller, R. J. D.; Muenter, A. A.; Parkinson, B. A. *J. Phys. Chem.* **1992**, *96*, 2820.

(13) Prezhdo, O. V.; Duncan, W. R.; Prezhdo, V. V. *Acc. Chem. Res.* **2008**, *41*, 339; *Prog. Surf. Sci.* **2009**, *84*, 30.

(14) Moser, J. E.; Wolf, M.; Lenzmann, F; Grätzel, M. *Z. Phys. Chem.* **1999**, *212*, 85.

(15) Sakata, T.; Hashimoto, K.; Hiramoto, M. *J. Phys. Chem.* **1990**, *94*, 3040.

(16) Li, Y. Z.; Zhao, X. H.; Li, H. X.; Jin, D. Z.; Ma, F. C.; Chen, M. D. *Mol. Phys.* **2009**, *107*, 2569.

(17) Tachibana, Y.; Rubtsov, I. V.; Montanari, I.; Yoshihara, K.; Klug, D. R.; Durrant, J. R. *J. Photochem. Photobiol., A* **2001**, *142*, 215.

(18) Katoh, R; Furube, A.; Hara, K.; Murata, S.; Sugihara, H.; Arakawa, H.; Tachiya, M. *J. Phys. Chem. B* **2002**, *106*, 12957.

(19) Huber, R.; Spörlein, S.; Moser, J. E.; Grätzel, M.; Wachtveitl, J. *J. Phys. Chem. B* **2000**, *104*, 8995.
(20) Nelson, J. *Phys. Rev. B* **1999**, *59*, 15374.
(21) Similar formula appeared in the derivation of tunneling current formula, e.g. Nguyen, H. Q.; Cutler, P. H.; Feuchtwang, T. E.; Miskovsky, N. *Surf. Sci.* **1984**, *146*, 405.
(22) Benkö, G.; Skårman, B.; Wallenberg, R.; Hagfeldt, A.; Sundström, V.; Yartsev, A. P. *J. Phys. Chem. B* **2003**, *107*, 1370.
(23) Ferber, J.; Stangle, R.; Luther, J. *Sol. Energy Mater. Sol. Cells* **1998**, *53*, 29.
(24) Chen, K. S.; Liu, W. H.; Wang, Y. H.; Lai, C. H.; Chou, P. T.; Lee, G. H.; Chen, K.; Chen, H. Y.; Chi, Y.; Tung, F. C. *Adv. Funct. Mater.* **2007**, *17*, 2964.
(25) Hara, K.; Sato, T.; Katoh, R.; Furube, A.; Ohga, Y.; Shinpo, A.; Suga, S.; Sayama, K.; Sugihara, H.; Arakawa, H. *J. Phys. Chem. B* **2003**, *107*, 597.
(26) Xu, W.; Peng, B.; Chen, J.; Liang, M.; Cai, F. *J. Phys. Chem. C* **2008**, *112*, 874.
(27) Santos, T. D.; Morandeira, A.; Koops, S.; Mozer, A. J.; Tsekouras, G.; Dong, Y.; Wagner, P.; Wallace, G.; Earles, J. C.; Gordon, K. C.; Officer, D.; Durrant, J. R. *J. Phys. Chem. C* **2010**, *114*, 3276.
(28) Minaev, B. F.; Minaeva, V. A.; Baryshnikov, G. V.; Girtu, M. A.; Agren, H. *Russian J. Appl. Chem.* **2009**, *82*, 1211.
(29) Heimer, T. A.; Bignozzi, C. A.; Meyer, G. J. *J. Phys. Chem.* **1993**, *97*, 11987.